Available online at www.sciencedirect.com

ScienceDirect

Physics Procedia 88 (2017) 258 – 265

Physics Procedia

8th International Topical Meeting on Neutron Radiography, Beijing, China, 4-8 September 2016

Samples to determine the resolution of neutron radiography and tomography

A.P. Kaestner[a,*], Z. Kis[b], M.J. Radebe[c], D. Mannes[a], J. Hovind[a], C. Grünzweig[a], N. Kardjilov[d], E.H. Lehmann[a]

[a]*Laboratory for Neutron Scattering and Imaging, Paul Scherrer Institut, CH-5232 Villigen – PSI, Switzerland*
[b]*Nuclear Analysis and Radiography Department, Centre for Energy Research, Hungarian Academy of Sciences, H-1525 Budapest 114, P.O. Box 49, Hungary.*
[c]*Radiation Science, NECSA, P1500, P.O Box 582, Pretoria, 0001, Republic of South Africa*
[d]*Institute Applied Materials, Helmholtz-Zentrum Berlin für Materialien und Energie, Lise-Meitner-Campus, Hahn-Meitner-Platz 1, D-14109 Berlin, Germany*

Abstract

Knowing the resolution and effective pixel size of an imaging system is essential for dimensional and quantitative measurements. A collection of test devices was developed for neutron imaging that can be used to quantify pixel and voxel size, resolution of the imaging system, and beam divergence. The first set of devices is intended for measurements with radiographs using test patterns or an absorbing edge. For tomography, Al vials were filled with Ti spheres of increasing dimensions in each vial. Ti was chosen since it provides sufficient contrast while the transmission is still guaranteed. The first resolution criterion was to determine from which vial that the spheres can be uniquely identified as spheres. More complex analysis would involve measuring the volume of the spheres or even to compute the edge spread function analogous to the method with the knife-edge for radiographs. For the edge analysis, a larger Ti sphere was considered. Using a sphere for the edge spread function analysis allowed for determination of the resolution in any direction. Images acquired using the different test items are included and methods to perform the analysis required to quantify the resolution from the images are proposed.

Peer-review under responsibility of the organizing committee of ITMNR-8

Keywords: Neutron imaging, Radiography, Computed Tomography, Resolution, Test devices, Image processing

1. Introduction

The resolution that can be achieved with a given imaging setup is a key parameter when the performance of the setup is described. The availability of a simple and efficient method to measure the resolution is of high importance for neutron imaging, in particular, as most installations are camera based with a variable field of view. This means that the resolution changes every time the field of view is changed and when the detector system is changed. The focusing procedure also requires feedback from the image sharpness. Different approaches have been proposed to determine

* Corresponding author. Tel.: +41-56-310-4286 ; fax: +41-56-310-3131.
E-mail address: anders.kaestner@psi.ch

Peer-review under responsibility of the organizing committee of ITMNR-8
doi:10.1016/j.phpro.2017.06.036

the resolution using X-rays some have even been standardized, e.g. the duplex wire method (ASTM, Standard No. D 2002-2015, 2015) and also detector characterization (ASTM, Standard No. E 2597M-2014, 2014). The most direct and rapid way to determine the resolution range is by using test patterns like line pairs or the Siemens star. We have produced test items using laser ablation to create these test patterns on Gd sputtered glass. The items are made with different dimensions and patterns. A different method to determine the resolution from radiographs is to use the edge response from a sharp edge (knife-edge) of a strongly absorbing material. Our knife-edge item is made of a Gd sheet mounted in an Al frame that makes the positioning easier. This item has a horizontal and vertical edge that can be used to determine the resolution in two directions. The beam divergence can also be determined using this item when it is placed at different distances from the detector. At Paul Scherrer Institut we have designed patterns based on the Siemens star as a tool to quickly observe and measure the current resolution of a neutron radiograph (Grünzweig et al., 2007).

Quantifying the resolution in computed tomography increases the complexity of the test device design. The third dimension adds the criteria that the sample must be able to transmit the radiation from all views of the tomography scan. A test device designed as a disc has been introduced for X-ray based CT in ASTM, Standard No. E 1695–1995 (2013). In this paper we propose two new test devices using spheres to determine the resolution. In collaboration with the International Atomic Energy Agency (IAEA) a set of samples for computed tomography was designed and will be evaluated in a round robin test cycle. In this paper we describe different samples with the purpose to determine the spatial resolution for radiography and computed tomography with neutrons.

2. Sample descriptions

2.1. Radiography

Radiography is the basic acquisition mode for a neutron-imaging instrument. The radiographs are either used directly or as raw information for more complex methods such as computed tomography, grating interferometry imaging, spectral imaging etc. The sharpness of the computed images produced by all these methods depends on the sharpness of the original radiographs. Therefore, it is of high importance to have an easy method to determine the resolution of the radiographs such that it is possible to measure the resolution conveniently for every change in experimental configuration. This is particularly important for camera based instruments with variable field of view (FOV) as the camera is refocused every time a new FOV is needed. We propose two different test devices to determine the resolution of a radiograph; 1) test patterns that indicate the resolution directly, Fig. 1, and 2) items to determine the sharpness of a high contrast edge, Fig. 2.

The large test pattern shown in Fig. 1 is made of a 5 μm Gd layer sputtered on a transparent glass substrate. This makes it possible to use the test pattern also with visible light for the first focusing, before being exposed to neutron radiation. The device contains four different feature types to the determine the spatial resolution. Siemens stars located at different places to verify if the resolution depends on the position on the detector. Line patterns with different line spacings from 0.010 mm to 1.0 mm were placed vertically and horizontally, Table 1.

Line width [mm]	0.01	0.025	0.05	0.75	0.1	0.2	0.3	0.5	1.0
Spatial frequency [lp/mm]	50	20	10	6.67	5	2.5	1.67	1	0.5

Table 1. Line widths present in the line patterns and their spatial frequencies.

A slanted box (tilt angle 3°) was included for measurements of the modulation transfer function (MTF). Finally, there are also line grids that can be used to measure the pixel size for the chosen FOV. There are grids with 1 mm and 10 mm line spacing. The lines in the grids can furthermore be used to identify lens distortion and provide information for a distortion correction procedure.

The second type of device is made of a Gd sheet with two polished edges mounted in a frame for convenient positioning. It provides an estimate of the resolution by means of an image analysis step to provide the resolution. The analysis steps for this test device are to determine the pixel size (variable if the FOV can be changed) and to measure the width of the edge spread function or the modulation transfer function (Boreman, 2001). This device can also be used to estimate the penumbra blurring at different distances from the detector. The procedure for this kind of

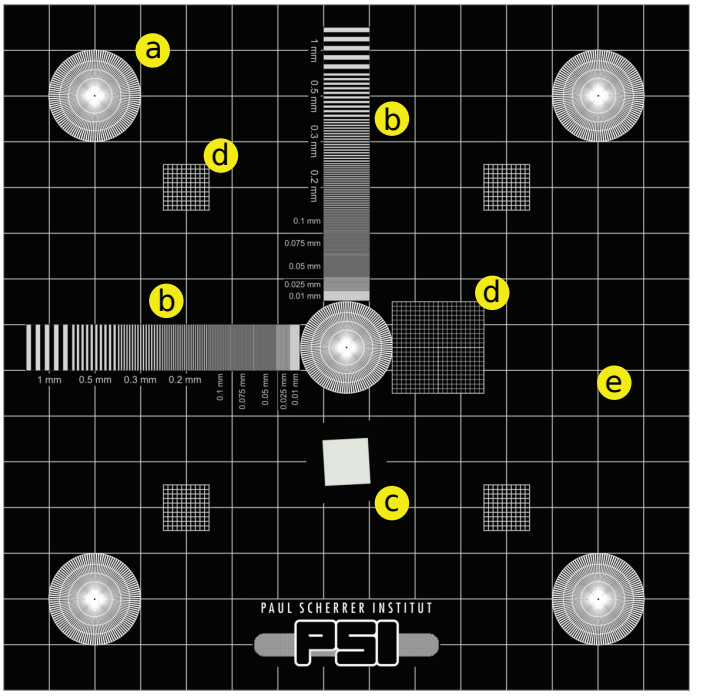

Fig. 1. Test pattern for neutron radiography. The pattern includes features to measure resolution (Siemens stars (a), line patterns (b), and a slanted edge box (c)), grids to determine pixel size, and geometric distortion (d and e).

measurement requires that the device is placed at different distances from the detector and that an image is acquired at each position. For this a distance frame can be used, Fig. 2b.

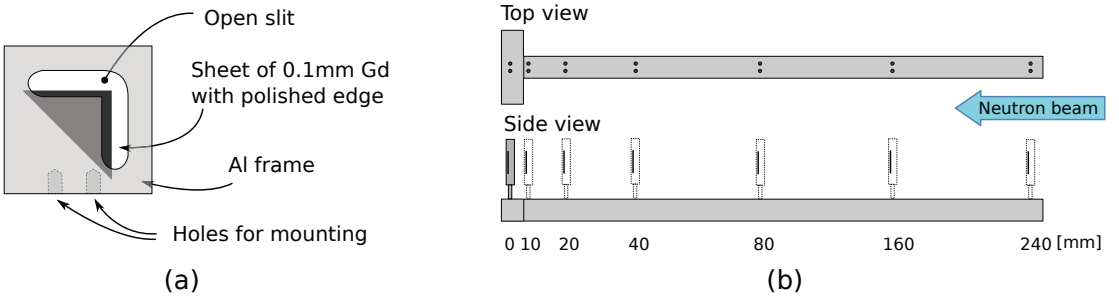

Fig. 2. Front view of the edge resolution device made of Gd to provide highest possible contrast (a). The edge is mounted in an Al frame with the dimensions 50×50×10 mm^3. The Gd sheet mounted in the frame has the side length 30 mm. Placing the device at different distances from the detector allows to estimate the collimation ratio. A distance frame (b) helps placing the resolution device at different distances as indicated by the shaded edge devices.

2.2. *Computed tomography*

The resolution of computed tomography of often lower than the resolution of the radiographs used as projections for the reconstruction, this is in particular true when filtered back projection is used to reconstruct the data. This is a consequence of the reconstruction filter and the interpolation during the back projection process. The data acquisition

required to quantify the CT resolution is a complete CT scan with the same conditions as intended for the following experiment. Thus, it is a time consuming procedure to measure the resolution of a CT. This will usually be avoided, unless it can be done in parallel with the experiment data acquisition. Quantifying the resolution in tomographic data is more challenging as it is difficult to design test patterns of items that have sufficiently high level of detail and at the same time also allows transmission of the radiation in any direction. The samples receive a considerable neutron dose during the CT scan. Therefore, sample activation should be considered to avoid long waiting times for the sample to deactivate. Considering these requirements, we propose to use sets of precision spheres, with each set with of different dimensions. We used the sphere diameters of 0.32 mm, 0.704 mm, 1.00009 mm, 2.092 mm, and 4.99 mm in our prototype set. The outcome using this type of sample would be a three-dimensional analogue to the duplex wire for radiographs. The resolution is determined by identifying the smallest sphere dimension that can be determined unambiguously, i.e. several vials each containing a different sphere dimension are required to define the resolution. These vials can be scanned as the main sample in a dedicated resolution experiment or they can be placed below or above the investigated sample. The second approach provides a resolution benchmark as part of the experiment and saves time.

To determine the resolution by means of the edge spread function or the MTF requires a high contrast edge in the reconstructed CT data. These are contradicting requirements as high contrast would result in detector starvation, which, in turn, would ruin the reconstructed data and produce unreliable edges, if any at all. The diameter of the sphere must be large compared to the voxel size, as the edge profile measurement requires an approximately flat surface, i.e. curvature less than one pixel. We chose to use spheres with the diameters of 10.004 mm and 20.001 mm as this will provide sufficiently large flat areas, even for pixel sizes of 0.5 mm. We consider this sufficient for most neutron imaging setups worldwide. Larger pixel sizes can still be handled if a larger sphere is chosen, but the transmission must be considered to avoid starvation effects in the projection data.

By inspecting the cross section data (Sears, 1992) for different elements, titanium was chosen as the best candidate in terms of attenuation and activation. It also has the feature that the edge effects caused by by the negative scattering length are visible for pixel sizes less than 20 μm and appear as a smoother edge response instead of introducing edge ripple.

3. Data processing

3.1. Radiography

The first step of the test pattern analysis is to determine the effective pixel size, which is done by using the linear grids in the background of the test device. The pixel size is obtained by measuring the number of pixels between two or several grid lines (mostly the ones with 10 mm spacing) and then dividing the metric distance by the number of pixels.

The analysis of test patterns is mainly done by extracting line profiles over the different line patterns. These profiles show the system response to different spatial frequencies as shown for the linear pattern in Fig. 3. The radiograph was acquired with an effective pixel size of 76.4 μm. The highest spatial frequency that can be observed unambiguously at this pixel size is 6.54 lp/mm. As shown in Table 1, the pattern with 0.1 mm (5 lp/mm) lines is the finest line pattern that can be resolved. This is confirmed by the profile plot and more clearly by the Fourier transform of the profile, which shows good response to a pattern at 5 lp/mm.

The edge images from the high contrast edge device can be evaluated either by determining the line spread function or the MTF. This information can be obtained using a single image or, when several images are acquired, by separating the two components of the total unsharpness. They are the detector blurring ($\sigma_{detector}$) and the penumbra blurring ($\sigma_{penumbra}$). Together, they contribute to the total unsharpness $\sigma_{precieved}$ as

$$\sigma_{percieved} = \sqrt{\sigma^2_{detector} + \sigma^2_{penumbra}} \tag{1}$$

The estimation procedure to find the two components is outlined in Appendix A. Fig. 4 shows edge images at different distances and the evaluation of the edge information.

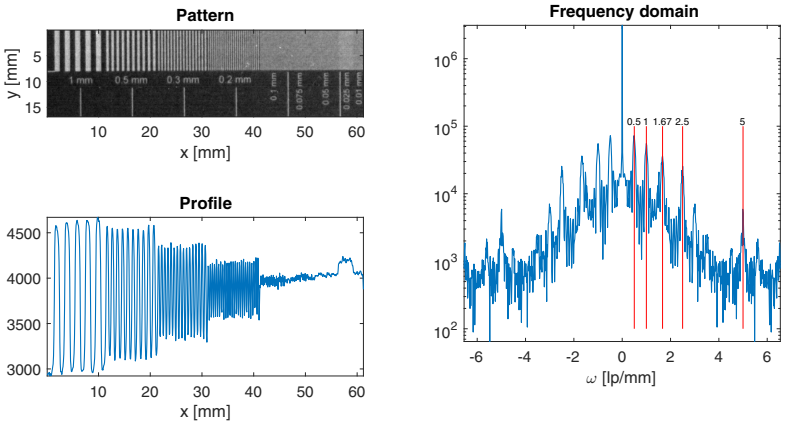

Fig. 3. A radiograph of the line pattern with vertical lines from the test device in Fig. (1) and the averaged horizontal profile that indicates the resolution of the current configuration. The Fourier transform of the profile show clear peaks for each resolved line patters. The red lines mark the spatial frequencies listed in Table (1) and coincide well with the resonance peaks.

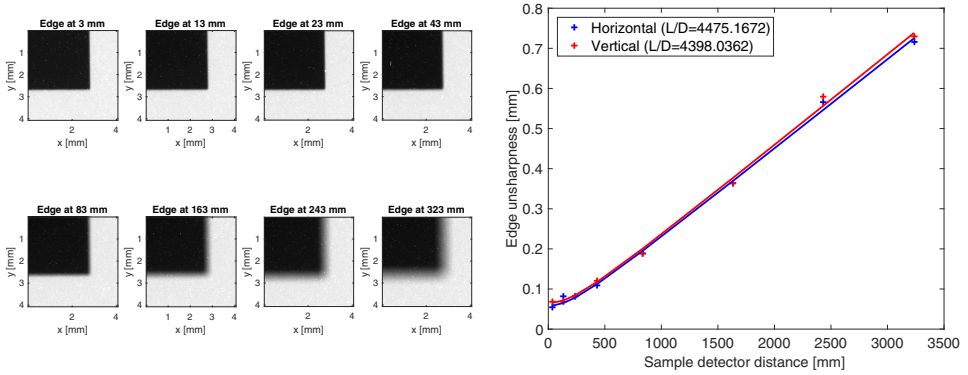

Fig. 4. Radiographs showing the edge response of a Gd edge placed at different positions from the detector. The image sequence was measured at ICON using the micro setup. The plot to the right shows the measured edge width and a fit as described in Appendix A.

3.2. Computed tomography

The third dimension makes the extraction of line profiles less reliable as it is hard to identify lines perpendicular to the object surface. Therefore, more advanced methods need to be considered. For the vials with spheres, the individual spheres have to be identified and their volume measured. This is done by first applying a threshold to produce a bilevel image that separates the spheres from the background. The spheres are presented as a single assembly in the bilevel images; however, for the analysis it is nescessary to identify the individual spheres. This is achieved using the watershed segmentation algorithm (Soille, 2002) after preparation of the bilevel image according to Kaestner et al. (2008). The watershed algorithm labels the spheres and makes it possible 1) to count the number of identified spheres and 2) to measure the sphere volume by counting the voxels per label. Fig. 5 shows images from the steps to calculate the volume of the spheres in the vial of 1 mm spheres. The procedure found that the average volume was 0.522 mm^3, the confidence intervals are marked in the measurement plot to the right in Fig. 5. This measurement is in agreement with the volume 0.524 mm^3, which was calculated using the equation for the sphere volume and the nominal sample radius. The low precision of the measurements is a consequence of the smooth edge and the low signal to noise ratio. This makes it difficult to define a threshold, in particular for noisy data. This procedure is therefore suited for analysis

of the robustness of the complete acquisition and processing chain. It would thus be beneficial for the precision to use a material that provide sharper edges, compare the sharpness of the vial wall.

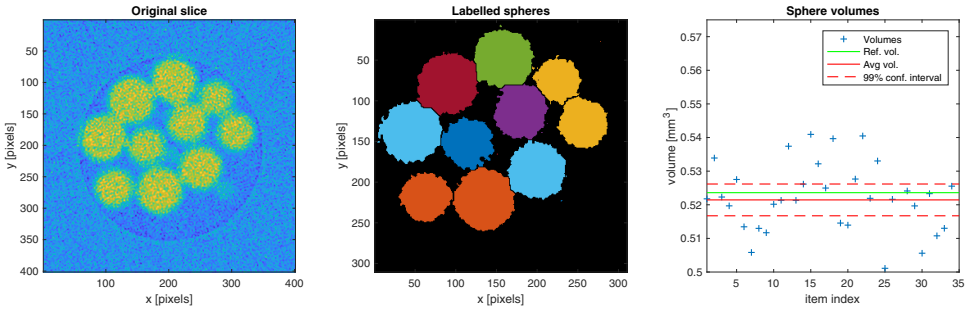

Fig. 5. Images showing different steps of the analysis work-flow to measure the sphere volumes in a vial. Volume measurements are plotted in the diagram to the right.

Spheres are attractive shapes as they are symmetric. It must however be noted that the shape is presented on a discrete grid with finite step sizes. The deviations from the expected volume can be considerable if the sphere is too small compared to the voxel size as shown in Fig. 6. Therefore, spheres with a radius of less than, say, 5-10 times the effective pixel size are not suitable objects to measure the 3D resolution for that specific imaging setup.

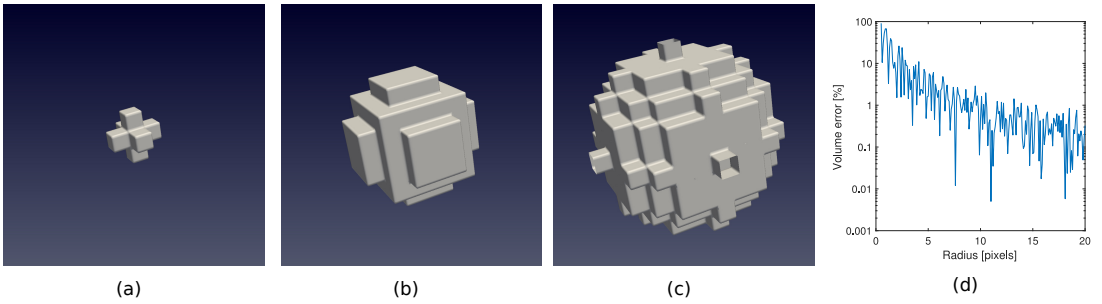

Fig. 6. Discrete spheres are bad approximations for small radii, (a)–(c) shows spheres with R=1,3.5, and 5. The plot in (d) show the percentual deviation in volume between the analytical and the discrete sphere.

The analysis steps for the 3D image, f, of the larger sphere aims at extracting the edge spread function, either globally isotropic or for selected solid angles. The preparation involves the steps of thresholding and cleaning of misclassified voxels to create a mask for the sphere. The mask is then eroded by a spherical structure element with a radius of W voxels. W is chosen for the expected width of the edge. Since erosion by large structure elements is time-consuming, therefore we used a distance map with a threshold at the distance W. The global edge spread function, p, is then computed as the expectation, $E[x]$, of the intensities across the edge

$$p(d) = E\left[f(i)\right] \quad \{i|i \in D(i) = d\} \tag{2}$$

where d is a list of all unique distance values in a distance map D. Usually, it makes sense to reduce the list to contain only values $d < 2\,W$ as distances beyond this limit do not contribute any information to the edge profile. This approach is demonstrated in Fig. (7) using the CT scan of a 20 mm Ti sphere, voxel size 45 μm.

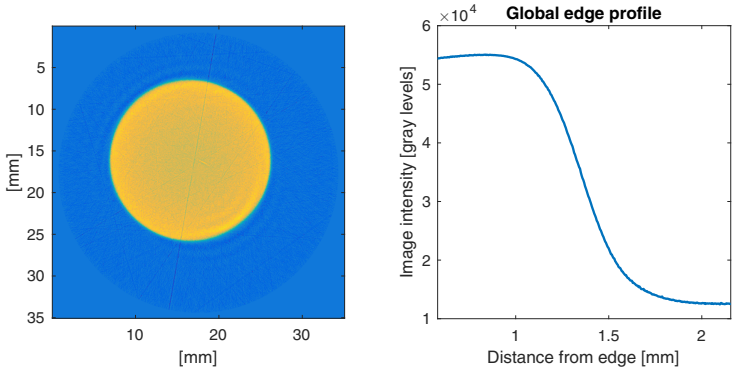

Fig. 7. Using a large Ti sphere to determine the unsharpness of the CT system. A slice is extracted from the CT data to show the unsharpness (left) to determine the global edge spread function (right).

4. Conclusions

A collection of samples, which can be used to measure the resolution of 2D (radiographs) and 3D (computed tomography) neutron images. These samples have been manufactured and tested at our neutron imaging beamlines to verify the response using different beam spectra and detector setups. Preliminary methods to analyze the resulting images have been outline. We chose spheres as geometry to determine the resolution of CT data. The sphere has the advantage that the operator cannot position the sample incorrectly due to the isotropic shape. The choice to use Ti as material for the 3D measurements should be verified with different materials to obtain the best contrast and edge sharpness.

Methods to determine the resolution on radiographs tend to measure the performance of the acquisition system. For computed tomography, results also include the performance of the following computational steps. In the edge analysis procedure consider the smoothing introduced by the reconstruction step in addition to the optical performance of the acquisition are considered.

With the development of high resolution imaging systems approaching pixel or voxel sizes in the order of a micron, it becomes more complicated to provide good test devices. While the creation of the devices require advanced equipment, the impact on edge enhancement becomes more prominent. The design of methods to handle such resolutions is important, but beyond the scope of this proposed set of test devices.

Acknowledgements

This work has been performed with the support from the IAEA. The authors would also like to thank Dr. Aaron Craft, Idaho National Labs, for interesting discussions.

Appendix A. Derivation of the estimate that separates detector and penumbra blurring

The measured edge spread mainly depends on two factors: 1) the detector PSF ($\sigma_{detector}$) and 2) the penumbra blurring ($\sigma_{penumbra}$). They are combined as $\sigma_{percieved} = \sqrt{\sigma^2_{detector} + \sigma^2_{penumbra}}$. The penumbra blurring is defined as $\sigma_{penumbra} = l\,\frac{D}{L}$ where L is the distance from aperture to the detector, D is the size of the aperture, and l is the sample to detector distance. Hence, we can see that there is one parameter changing with the sample detector distance while the other is constant i.e.

$$\sigma_{percieved}(l)^2 = \sigma^2_{detector} + (l\,\sigma_{penumbra})^2 \tag{A.1}$$

For several measurements, this can be formulated as a system of linear equations

$$\begin{aligned}\sigma^2_{detector} + (l_1\,\sigma_{penumbra})^2 &= \sigma^2_1\\ \sigma^2_{detector} + (l_2\,\sigma_{penumbra})^2 &= \sigma^2_2\\ &\vdots\\ \sigma^2_{detector} + (l_N\,\sigma_{penumbra})^2 &= \sigma^2_N\end{aligned} \tag{A.2}$$

this can be written in matrix form as

$$\underbrace{\begin{bmatrix}1 & l_1^2\\ 1 & l_2^2\\ \vdots & \vdots\\ 1 & l_N^2\end{bmatrix}}_{H} \underbrace{\begin{bmatrix}\sigma^2_{detector}\\ \sigma^2_{penumbra}\end{bmatrix}}_{\theta} = \underbrace{\begin{bmatrix}\sigma^2_1\\ \sigma^2_2\\ \vdots\\ \sigma^2_N\end{bmatrix}}_{x} \tag{A.3}$$

i.e. the least squared solution would be $\theta = (H^T\,H)^{-1}\,H^T\,x$. This estimate would provide a more or less straight line that is missing the knee of the mixing between $\sigma_{detector}$ and $\sigma_{penumbra}$. We propose to introduce a weighting function proportional to the inverse of the sample-detector distance to force the estimate to focus on short distance values (near the knee) more than on remote values (straight line proportional to L/D) as the most interesting part of the curve is close to the detector. The weight matrix takes the form

$$W = \begin{bmatrix}1/l_1 & 0 & \cdots & 0\\ 0 & 1/l_2 & \cdots & 0\\ \vdots & \vdots & \ddots & \vdots\\ 0 & 0 & \cdots & 1/l_N\end{bmatrix} \tag{A.4}$$

and the estimate now takes the form

$$\theta = (H^T\,W\,H)^{-1}\,H^T\,W\,x \tag{A.5}$$

The two unsharpness components are given by the elements of θ as $\sigma_{detector} = \sqrt{\theta_1}$ and $\sigma_{penumbra} = \sqrt{\theta_2}$

References

ASTM, Standard No. D 2002-2015, 2015. Standard practice for determining total image unsharpness and basic spatial resolution in radiography and radioscoy. doi:10.1520/E2002-15.

ASTM, Standard No. E 1695–1995, 2013. Standard test method for measurement of computed tomography (ct) system performance. doi:10.1520/E1695-95R13.

ASTM, Standard No. E 2597M-2014, 2014. Practice for manufacturing characterization of digital detector arrays. doi:10.1520/E2597_E2597M-14.

Boreman, G., 2001. Modulation Transfer Function in Optical and Electro-Optical Systems. SPIE, Bellingham, USA. doi:10.1117/3.419857.

Grünzweig, C., Frei, G., Lehmann, E., Kühne, G., David, C., 2007. Highly absorbing gadolinium test device to characterize the performance of neutron imaging detector systems. Review of Scientific Instruments 78, 053708. doi:10.1063/1.2736892.

Kaestner, A., Lehmann, E., Stampanoni, M., 2008. Imaging and image processing in porous media research. Advances in Water Resources 31, 1174–1187. doi:10.1016/j.advwatres.2008.01.022.

Sears, V., 1992. Neutron scattering lengths and cross sections. Neutron News 3, 26–37. doi:10.1080/10448639208218770.

Soille, P., 2002. Morphological image analysis. 2nd ed., Springer Verlag.